

Radiated Spurious Emission Prediction Based on Dipole Moment and Full Wave Simulation

Qiaolei Huang, Jagan Rajagopalan, Duck Ho Bae, Akshay Mohan and Deepak Pai

Amazon Lab126, 1100 Enterprise Way, Sunnyvale, CA, USA

Abstract— In this paper, an equivalent dipole moment method and full wave simulation are proposed to predict radiated spurious emissions (RSE). The proposed method is utilized in design of a practical electronic device. Based on near field patterns, the radiation physics of 2.4GHz Wi-Fi transmitter harmonics in the device is identified to be a magnetic dipole moment. Reduction of loop size is proved to be an effective method to reduce RSE of 2.4 GHz. In addition, RSE of 5 GHz Wi-Fi transmitter is simulated using a full wave solver and methods to reduce RSE are discussed. Measured RSE results are also shown to validate proposed prediction and mitigation methods.

Keywords—RSE, emission, dipole moment, near field to far field

I. INTRODUCTION

With rapid growth of wireless connectivity integrated circuits (ICs), more and more radio systems are integrated to a single electronic device. In addition, as the data rate and clock frequency of IC continue to increase, risk to failures observed from electromagnetic compatibility (EMC) and radio frequency interference (RFI) are high. In the past, researchers have proposed both simulation-based and measurement-based method in order to solve EMC and RFI problems. In [1]-[3], simulation tools are used to understand radiating noise sources and how near field and far field contribute to EMC and RFI failures. In [4]-[7], near field scanning measurements are used to build equivalent radiation models.

This paper describes an approach that uses simulation based method and near field measurement method to predict and mitigate radiated spurious emissions (RSE) problems. Radiated spurious emissions are defined as the unwanted radiated emission on frequency range which are outside regions of intended operational frequency of any communication radio system. Harmonic radiations of a transmitter line up are often the strongest contributors to RSE. Harmonic signals are generated by non-linear components, such as, mixer, power amplifier, etc. which are radiated by metal structures within the electronic device, such as heatsinks, cables or antennas. Government bodies strictly regulate RSE level. For example, in US, consumer electronic devices need to pass RSE test limits before going to market according to FCC part 15.

There are a few methods to reduce RSE. In [8], researchers use a quarter-wavelength open stub to reduce RSE on a test board setup. Frequency-Selective Surface is used in [9] to reduce RSE from a spiral inductor. Band-stop characteristic of

split ring resonators are used in [10] to suppress spurious radiations of a patch antenna. Defective ground structures is used in [11] to suppress spurious radiations of a microstrip patch antenna.

In this paper, we first propose dipole moment method to predict RSE for a practical design of electronic device, as shown in Figure 1. By understanding the radiation physics, RSE reduction methods are also discussed.

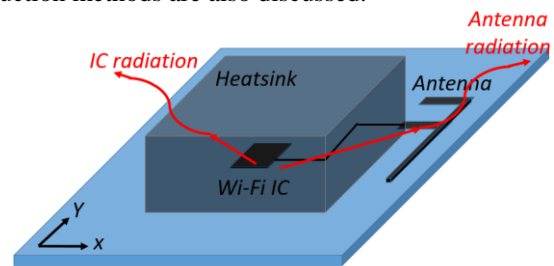


Figure 1. RSE radiation possibilities in the device.

The paper is organized as below. Section II discusses the RSE prediction method based on equivalent dipole moment and full wave simulation. Section III discusses the RSE prediction and reduction for harmonics of 2.4GHz Wi-Fi. RSE simulation and reduction for harmonics of 5GHz Wi-Fi are covered in Section IV. Section V provides conclusion and future direction.

II. RSE PREDICTION

In [12]-[14], an array of electric and magnetic dipole moments can be equivalently chosen to fit the measured near field data. The following linear relationship between the measured H-field and the dipole moment sources can be established.

$$\begin{bmatrix} [H_x]_{K \times 1} \\ [H_y]_{K \times 1} \end{bmatrix} = [T]_{2K \times 6N} \begin{bmatrix} [P_x]_{N \times 1} \\ [P_y]_{N \times 1} \\ [P_z]_{N \times 1} \\ [M_x]_{N \times 1} \\ [M_y]_{N \times 1} \\ [M_z]_{N \times 1} \end{bmatrix} \quad (1)$$

where K is the number of the measured points on the near field scanning plane. N is the number for each type of dipole moment. H_x and H_y are measured H fields at each of K measured points. Each element in the T matrix denotes the contribution of

one type of the dipole moment to one component of the magnetic field. T can be easily obtained once the locations of the observations plane and the dipole moment source are known [13]. (1) can also be simplified as

$$F = T \times X \quad (2)$$

where F is the measured H fields with the size of $2K \times I$. T is the transfer function with the size of $2K \times 6N$. Moreover, X is the unknowns for all of the electric and magnetic dipole moments with the size of $6N \times I$. The least square method is applied here to solve the inverse problem. The solution is

$$X = (T^T T)^{-1} T^T F \quad (3)$$

As long as the noise source dipole moments can be obtained correctly, the dipole moments can be imported into the full 3D model of the device to estimate far field RSE. Equation (3) serves a general method to obtain equivalent dipole moments for any radiation source, while in many cases, only one or a few dipole moments are needed to represent a noise source, as shown in [5], [12] and [14].

III. RSE RADIATION FOR 2.4GHZ WI-FI

The electronic device in this study supports 2.4 GHz /5 GHz Wi-Fi in a single WLAN IC. Without a shield can on IC, as shown in the simplified picture in Figure 1, RSE from this device is attributed to 2 components: (1) harmonic power from IC itself, which is then transmitted to device antenna and radiate out; (2) WLAN IC noise couples to nearby heatsink or other structures that radiates out. RSE from component (1) is typically calculated by the conducted harmonic values in conjunction with antenna gain at harmonic frequencies. In this particular sample, it is observed that RSE data with shield can meets RSE spec with 20 dB margin which leads to the conclusion that component (1) radiation in this device can be ignored. Part (2) is the dominant component, which originates from the IC itself. Understanding the fundamental physics for IC radiation is the key. Note that the term ‘‘IC radiation’’ includes radiation from IC itself and its nearby traces.

Near field EM scanning was performed at $2f_0$ of 2.437GHz, which is 4.874GHz. H field patterns at 4.874GHz are shown in Figure 2. According to [12], there are 6 types of dipole moments, which are basic radiation sources. The electric dipole moment consists of an infinitely small electric current segment, denoted as P dipole moment. By duality, magnetic dipole moment is an infinitely small magnetic current segment, denoted as an M dipole moment. An infinitely small magnetic current segment is actually an infinitely small electric current loop. For a magnetic dipole moment, the direction is defined as the perpendicular direction to the plane of the electric current loop. For example, an M_y dipole moment denotes the magnetic current going toward the y -direction, where the electric current loop is in the xz plane. Based on orientations, there are six types of basic dipole moments: P_x, P_y, P_z, M_x, M_y and M_z . For the basic dipole moments, near and far fields can be calculated from the analytical formulas given in [13]. Thus, near field patterns

above the noise source can be analytically calculated. The near field patterns for all six dipole moments are shown in Figure 3. Figure 3 can serve as a look up table to identify dipole moment type based on near field scanned results.

The measured magnitude of H_x and H_y above the noise source as shown in Figure 2 corresponds to fifth dipole moment(dipole moment M_y) in Figure 3. H_x shows a butterfly shape. H_y shows three concentric circle shapes which has the strongest one in center. When the entire board is scanned, the near field radiation near the IC output region is the dominant part. Dipole moment M_y is the current loop in xz plane, the normal direction of the current loop is facing y . As shown in Figure 4, current at 4.874 GHz goes from the IC pin, hits the low pass filter components and the majority of the current from 4.874 GHz will return through the shunt path in z direction, thus forming a current loop in xz plane. In [14], researchers observed similar magnetic dipole moment radiation from CPU and DDR noise sources.

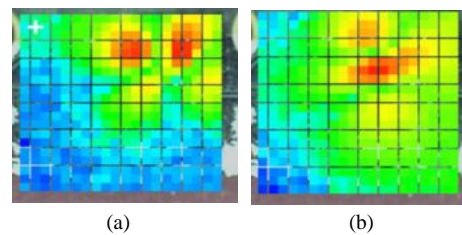


Figure 2. EM scanning of the IC radiation at $2f_0$ of 2.4 GHz Wi-Fi channel 6: (a) $|H_x|$ of 4.874GHz; (b) $|H_y|$ of 4.874GHz

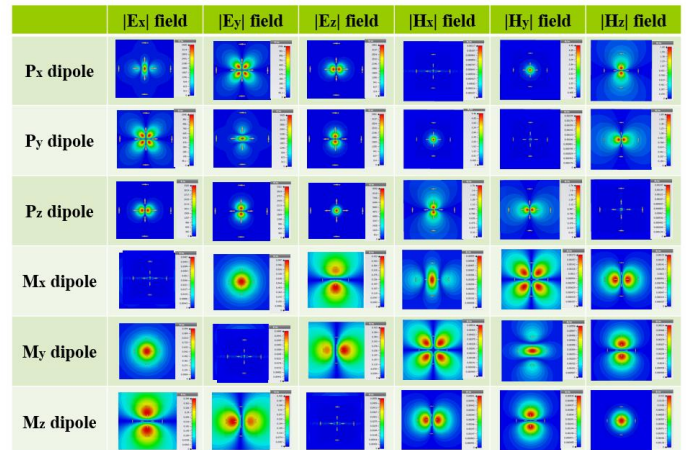


Figure 3. Magnitude of H and E field components from 6 dipole moments

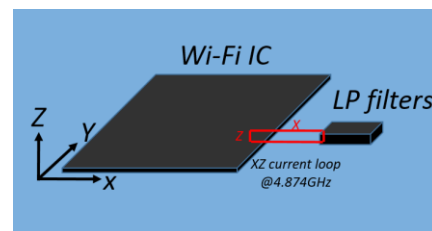


Figure 4. Radiation source is a current loop in xz plane for 4.874GHz.

The magnitude of magnetic dipole moment $M_y = I * S$. We can assume that the current on the loop can be approximated as constant. I is the constant current value at 4.874GHz from the Wi-Fi chip based on the fact that the wavelength at 4.874GHz in free space is 6.2cm and the length and width of the current loop is smaller than 1/10 of the wavelength. I is the constant current value at 4.874GHz from the Wi-Fi chip. S is the loop area. $S = L * h$. L is the length from IC Wi-Fi pin (inside IC) to the low pass filter. h is the height from first layer trace to second layer ground.

As the dominant radiation source is a single dipole moment M_y from the measured H field in Figure 2, the calculation process to obtain equivalent dipole moment M_y can be significantly simplified. By putting the equivalent dipole moment into the full model, RSE can be simulated with far field E field probes placed 3 meter away. In Figure 5(a), current loop in xz plane is used to replace the equivalent radiation source dipole moment M_y . Dipole moment M_y is the only radiation source in this model. There is no source excitation on the PCB as it's replaced by dipole moment M_y . The simulated far field RSE is 49.1 dBuV/m at 4.874 GHz. The measured RSE is 55.3 dBuV/m at 4.874 GHz. The observed delta is 6.2dB. The delta between the simulation and the measurement may be contributed by the following components. Firstly, the distance from the equivalent dipole moment M_y to the PCB ground plane below and the distance from the equivalent dipole moment M_y to the heatsink above are important factors and sensitive to accurate measurement in order to determine RSE. The simulated distances can be slightly different compared to actual measurements. Secondly, the equations in (1) and (2) assume that the dipole moment is above an infinite solid ground plane, however, actual PCB has finite size and it's not a solid ground plane. Lastly, the H field probe calibration can also introduce errors in H field measurements and also z direction variation. Overall, the dipole moment and full wave solver can be used to predict RSE within a certain error bound. In addition, it can help derive ways to reduce RSE.

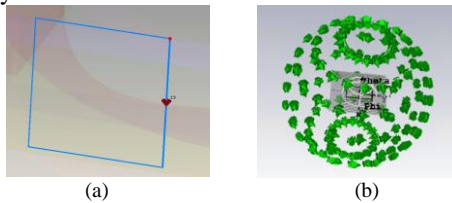


Figure 5. (a) Dipole moment M_y to replace the actual radiation source on the PCB, current loop in xz plane to replace the equivalent radiation source dipole moment M_y ; (b) far field probes at 3 meter distance.

To reduce RSE, the magnitude of dipole moment M_y need to be reduced. A layout change to shorten the loop area S is done to reduce RSE. With new layout, S is reduced to roughly one third of original. In theory, 9.5 dB magnitude reduction of dipole moment M_y will lead to RSE reduction of similar value. The measured RSE reduces by 7 dB, which is roughly within theoretical expectation.

Full wave simulation of the whole device is performed to capture far field RSE reduction in simulation. Figure 6 shows that simulated RSE from the updated layout change improves

by ~6 dB. Therefore, RSE reduction from simulation, theoretical and empirical data converges as expected.

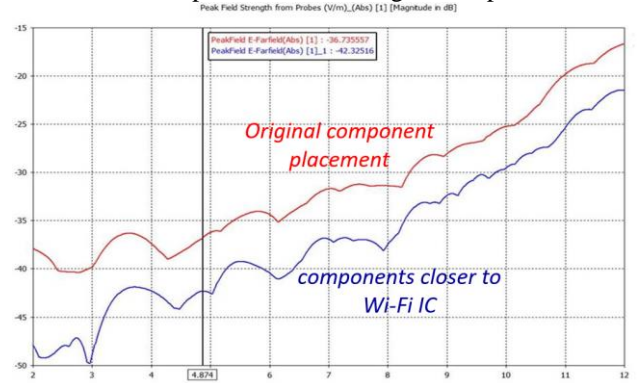


Figure 6. Simulated RSE improvement for $2f_0$ of 2.4GHz Wi-Fi. Relative RSE reduction is around 6dB.

IV. RSE RADIATION FOR 5 GHZ WI-FI

For $2f_0$ of 5GHz Wi-Fi, near field scanning is done across the board. Similar to the near field measurement of 2.4GHz harmonics, high pass filters were placed right after the H field probe to pass $2f_0$ and reject the high power fundamental f_0 . The near field radiation for H field of 10.36GHz is shown in Figure 7. The radiation physics is not dipole moment M_y . Based on locations of hot spots, the dominant radiation is identified as the exposed power supply traces on the first layer of the PCB.

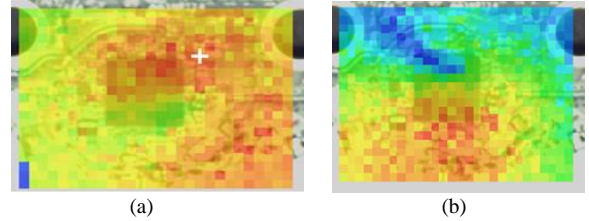


Figure 7. EM scanning of the IC radiation at $2f_0$ of 5 GHz Wi-Fi channel 36: (a) $|H_x|$ of 10.36GHz; (b) $|H_y|$ of 10.36GHz

A few methods are applied in the simulation to reduce the power trace radiation by changing components on the board. The simulated RSE reduction is shown in Figure 8.

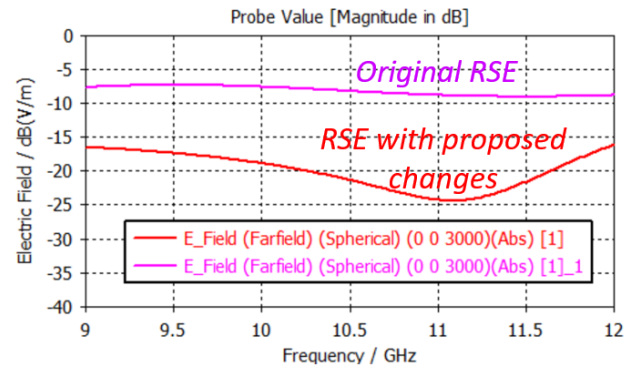


Figure 8. Relative RSE reduction for $2f_0$ of 5GHz Wi-Fi.

In order to validate the applied RSE reduction method in simulation, measurements were also performed and the

measured RSE reduction observed was 13 dB which also supports the simulation data.

V. CONCLUSION

In this paper, we propose methods to predict radiated spurious emission using equivalent dipole moments and full wave simulations. We applied this method to predict and mitigate RSE in a real electronic device. This device supports 2.4 GHz and 5 GHz Wi-Fi. For the 2.4 GHz Wi-Fi path, second harmonic radiation physics is dominated by a magnetic dipole moment. Thus reducing the loop size is used to mitigate RSE. On 5 GHz Wi-Fi path, second harmonic radiation physics is dominated by power trace radiation. Simulation is used to identify possible RSE reduction methods. Measured RSE results are also shown to validate proposed prediction and mitigation methods. The future work includes: deep understanding of the physics for power trace radiation; accurate modeling for radiation sources with complex near field patterns.

REFERENCES

- [1] Y. Wang et al., "A Simulation-Based Coupling Path Characterization to Facilitate Desense Design and Debugging," in Proc. of IEEE Symp. Electromagn.Compat., 2018, pp. 150-155.
- [2] C. Hwang and Q. Huang, "IC placement optimization for RF interference based on dipole moment sources and reciprocity," *2017 Asia-Pacific International Symposium on Electromagnetic Compatibility (APEMC)*, Seoul, 2017, pp. 331-333.
- [3] Q. Huang et al., "Accurate Prediction and Mitigation of EMI from High-Speed Noise Sources using Full Wave Solver," in Proc. of IEEE Symp. Electromagn.Compat., 2019, pp. 595-599
- [4] G. Shen, S. Yang, J. Sun, S. Xu, D. J. Pommerenke and V. V. Khilkevich, "Maximum Radiated Emissions Evaluation for the Heatsink/IC Structure Using the Measured Near Electrical Field," in *IEEE Transactions on Electromagnetic Compatibility*, vol. 59, no. 5, pp. 1408-1414, Oct. 2017
- [5] Q. Huang, T. Enomoto, S. Seto, K. Araki, J. Fan and C. Hwang, "A Transfer Function Based Calculation Method for Radio Frequency Interference," in *IEEE Transactions on Electromagnetic Compatibility*, vol. 61, no. 4, pp. 1280-1288, Aug. 2019.
- [6] Y. Sun, B. Tseng, H. Lin and C. Hwang, "RFI Noise Source Quantification Based on Reciprocity," in Proc. of IEEE Int. Symp. Electromagn.Compat., 2018, pp. 548-553
- [7] Q. Huang, T. Enomoto, S. Seto, K. Araki, J. Fan and C. Hwang, "Physics-Based Dipole Moment Source Reconstruction for RFI on a Practical Cellphone," *IEEE Trans. Electromagn. Compat.*, vol. 59, no. 6, pp. 1693-1700, Dec. 2017.
- [8] T. Koo, H. Lee, J. Yook, K. Yoo, J. Cheon and S. Lee, "Radiated spurious emission reduction using parasitic element for mobile applications," in Proc. of IEEE Int. Symp. Electromagn.Compat., 2014, pp. 760-764.
- [9] C. Chiu, Y. Chang, H. Hsieh and C. H. Chen, "Suppression of Spurious Emissions From a Spiral Inductor Through the Use of a Frequency-Selective Surface," *IEEE Trans. Electromagn. Compat.*, vol. 52, no. 1, pp. 56-63, Feb. 2010.
- [10] J.-G. Lee and J.-H. Lee, "Suppression of spurious radiations of patch antenna using split ring resonators (SRRs)," in Proc. IEEE Antennas Propag. Soc. Int. Symp., vol. 2B, pp. 242-245. July 2005.
- [11] H. Liu, Z. Li, X. Sun, and J. Mao, "Harmonic Suppression with Photonic Bandgap and Defected Ground Structure for a Microstrip Patch Antenna," *IEEE Microw. Wireless Compon. Lett.*, vol. 15, no. 2, pp. 55-56, Feb. 2005.
- [12] Q. Huang and J. Fan " Machine Learning Based Source Reconstruction for RF Desense," *IEEE Trans. Electromagn. Compat.*, vol. 60, no. 6, pp. 1640-1647, Dec. 2018.
- [13] Z. Yu, J. A. Mix, S. Sajuyigbe, K. P. Slattery, and J. Fan, "An improved dipole-moment model based on near-field scanning for characterizing near-field coupling and far-field radiation from an IC," *IEEE Trans. Electromagn. Compat.*, vol. 55, no. 1, pp. 97-108, Feb. 2013
- [14] Q. Huang et al., "Desense Prediction and Mitigation from DDR Noise Source," in Proc. of IEEE Int. Symp. Electromagn.Compat., 2018, pp. 139-144.